Fail-Safe Joints between Copper Alloy (C18150) and Nickel-Based Superalloy (GH4169) Made by Transient Liquid Phase (TLP) Bonding and Using Boron-Nickel (BNi-2) Interlayer

Journal Item

metals

MDPI

Article

Fail-Safe Joints between Copper Alloy (C18150) and Nickel-Based Superalloy (GH4169) Made by Transient Liquid Phase (TLP) Bonding and Using Boron-Nickel (BNi-2) Interlayer

Chengcong Zhang [1,2,*] and Amir Shirzadi [3,4]

1 International Research Institute for Steel Technology, School of Sciences, Wuhan University of Science and Technology, Wuhan 430081, China
2 Technical Centre, Shanghai Aerospace Equipment Manufacturer, Shanghai 200245, China
3 School of Engineering & Innovation (STEM), The Open University, Milton Keynes MK7 6AA, UK; a.shirzadi@open.ac.uk
4 School of Materials and Metallurgy, Wuhan University of Science and Technology, Wuhan 430081, China
* Correspondence: zhangcc0202@163.com; Tel.: +86-139-1836-8224

Abstract: Joining heat conducting alloys, such as copper and its alloys, to heat resistant nickel-based superalloys has vast applications in nuclear power plants (including future fusion reactors) and liquid propellant launch vehicles. On the other hand, fusion welding of most dissimilar alloys tends to be unsuccessful due to incompatibilities in their physical properties and melting points. Therefore, solid-state processes, such as diffusion bonding, explosive welding, and friction welding, are considered and commercially used to join various families of dissimilar materials. However, the solid-state diffusion bonding of copper alloys normally results in a substantial deformation of the alloy under the applied bonding load. Therefore, transient liquid phase (TLP) bonding, which requires minimal bonding pressure, was considered to join copper alloy (C18150) to a nickel-based superalloy (GH4169) in this work. BNi-2 foil was used as an interlayer, and the optimum bonding time (keeping the bonding temperature constant as 1030 °C) was determined based on microstructural examinations by optical microscopy (OM), scanning electron microscopy (SEM), energy dispersive spectrometry (EDS), tensile testing, and nano-hardness measurements. TLP bonding at 1030 °C for 90 min resulted in isothermal solidification, hence obtained joints free from eutectic phases. All of the tensile-tested samples failed within the copper alloy and away from their joints. The hardness distribution across the bond zone was also studied.

Keywords: transient liquid phase (TLP) bonding; joining; copper alloy; nickel-based superalloy; interlayer

Citation: Zhang, C.; Shirzadi, A. Fail-Safe Joints between Copper Alloy (C18150) and Nickel-Based Superalloy (GH4169) Made by Transient Liquid Phase (TLP) Bonding and Using Boron-Nickel (BNi-2) Interlayer. *Metals* **2021**, *11*, 1504. https://doi.org/10.3390/met11101504

Academic Editor: Andreas Chrysanthou

Received: 21 August 2021
Accepted: 20 September 2021
Published: 23 September 2021

1. Introduction

The combination of heat conducting materials (i.e., copper alloys) and high-temperature structural materials (i.e., stainless steel or nickel-based superalloys) is of great interest to the manufacturers of nuclear power plants and liquid propellant launch vehicles [1,2]. However, it is difficult to fusion weld copper alloys to high-nickel stainless steel or nickel-based superalloys due to their vulnerability to hot cracking, lack of adequate mixing, and formation of brittle intermetallics. Therefore, solid-state processes, such as diffusion bonding, are the preferred joining techniques [3–5].

Previous work has shown that copper alloys and nickel superalloys were successfully joined by solid-state diffusion bonding at the cost of imposing substantial deformation in copper alloys [6]. Such large deformations are not tolerable when near-net-shape manufacturing. Transient liquid phase (TLP) bonding is an attractive technique owing to the formation of liquid phase, which eliminates the need to apply large bonding pressures. In short, the absence of distortion and deformation in the parent materials is the main advantage of the TLP bonding process compared to solid-state bonding processes [7–9]. In

this process, an interlayer containing melting point depressant (MPD) elements such as B, Si, and P was used to form a liquid at the joint interface well below the melting point of base material [10].

On a basic level, the TLP bonding process involves four stages: (1) liquidation of the interlayer occurs at a certain temperature; (2) concentration of the MPD element in the liquid phase declines as it diffuses into the materials being joined; (3) depletion of the MPD element results in isothermal solidification and formation of a solid bond; and finally, (4) further solid-state homogenization redistributes the MDP and other elements uniformly on and around the bond line [8,11–13]. Among various bonding parameters, temperature, holding time, and interlayer are the main factors to affect the process outcome. Bonding temperature is normally selected between the liquidus temperature of the interlayer and the solidus temperature of the material with the lower melting point, i.e., copper alloy in this work. A sufficient holding time is necessary to complete the isothermal solidification and avoid formation of eutectic phases in the centreline, which can have adverse effects on mechanical properties of the joint [9,14–17]. For instance, S. Hadibeyk obtained complete isothermal solidification at 1130 °C within 100 min in dissimilar TLP bonded Ni-based GTD-111 and Co-based FSX-414 superalloys [15]. Akbar also reported complete isothermal solidification at 1050 °C for 45 min and 1100 °C for 30 min in dissimilar TLP-bonded IN718/IN600 joints using a BNi-2 interlayer [7]. Pouranvari obtained an isothermal solidification zone (ISZ) in an IN718 superalloy, which consisted of a single phase, by combining TLP bonding with standard heat treatment processes [18].

Although the TLP bonding of similar or dissimilar superalloys using BNi-2 interlayers has been well studied, reports on the TLP bonding of copper alloys to Ni-based superalloys are scant. In this work, TLP bonding of a copper alloy to a nickel superalloy was successfully achieved using a BNi-2 interlayer, and the influence of holding time on the microstructure and mechanical properties of the joints were investigated.

2. Materials and Methods

Copper alloy (C18150) and Ni-based superalloy (GH4169) were selected as the base materials, and a 30 μm thick amorphous BNi-2 foil was used as the filler metal in this work. The compositions of all materials are given in Table 1.

Table 1. Chemical compositions (wt. %) of parent and filler materials.

Materials	Cu	Ni	Cr	Fe	Ti	Nb	Mo	Zr	Si	B
C18150	Bal.	-	0.80	0.50	-	-	-	0.10	-	-
GH4169	-	Bal.	18.19	17.34	1.22	4.29	2.44	-	-	-
BNi-2	-	Bal.	7	3	-	-	-	-	4.5	3.2

The faying surfaces were prepared by conventional grinding techniques with a final 1200-grit finish followed by polishing with a 1μm polycrystalline diamond suspension. The post-polishing surface roughness and flatness were Ra 0.05–0.025 and 0.01/20 mm, respectively. The surface treatment used in this work requires conventional mechanical grinding and polishing techniques that can be applied on an industrial level. The parent and filler materials were both ultrasonically cleaned in an acetone bath and were then dried in air before inserting them into the purpose-built steel fixture shown in Figure 1. The fixture is made of 30CrMnSiA structural steel, and the bonding pressure was imposed simply by tightening the bolts to ensure a full contact between all of the parts.

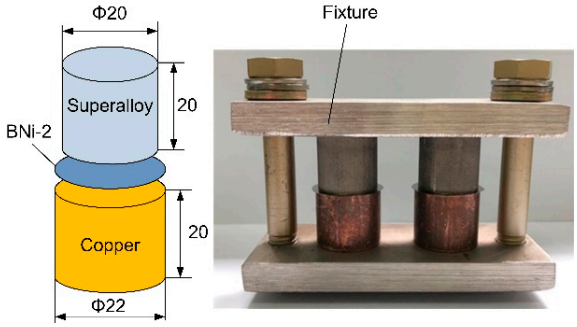

Figure 1. Dimensions (mm) and bonding setup of test specimens.

The melting points of the copper alloy and Ni-superalloy are 1073 °C and 1260 °C, respectively. The bonding temperature of all of the samples was 1030 °C, which is 31 °C above the liquidus temperature of BNi-2 (999 °C) and yet well below the melting point of the copper alloy. The bonding times were 30 min, 60 min, and 90 min, which were selected based on earlier trials and previous reports on bonding copper alloys to steels. A vacuum furnace operating at 1×10^{-3} Pa (1×10^{-5} mBar) and equipped with a radiation heating system was used to heat the samples at the rate of 10 °C/min followed by slow furnace-cooling down to ambient temperature. The cooling time from the bonding temperature to ambient temperature was about 10 h.

The bonded samples were cut along the longitudinal direction and were prepared by conventional metallography techniques. Each metallography sample was etched twice using two different etchants. The copper side was etched in a solution of 5 g $FeCl_3$ + 10 mL HCl + 100 mL water, whereas the nickel side was etched by a solution of 1 mL H_2SO_4 + 20 mL HCl + 4 g $CuSO_4 \cdot H_2O$ + 20 mL water, both at ambient temperature for 20 to 30 s.

The microstructure and composition of the bonded interface were examined using optical and scanning electron microscopes (SEM) equipped with an energy dispersive spectrometer (EDS).

Nano-hardness measurements were conducted across the bond line of the joint under 8 mN load and at 0.1 mN/s loading rate. Longer samples were also TLP bonded and machined for tensile testing using a universal testing machine—see Figure 2 for more details.

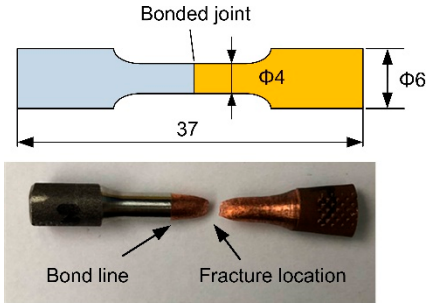

Figure 2. Dimensions (mm) and actual tensile-tested sample, which failed in copper alloy.

3. Results and Discussion

3.1. Microstructural Examinations

It has been well established that a typical TLP bonded joint may consist of three distinct zones: (1) an athermal solidification zone (ASZ), (2) an isothermal solidification zone (ISZ), and (3) a diffusion-affected zone (DAZ) [7,17,19–21]. Figure 3a shows the microstructure of a copper/nickel-superalloy sample TLP-bonded at 1030 °C for 60 min. The main zones of the joint are illustrated in the backscattered electron (BSE) micrograph with a higher magnification (Figure 3b). It appears that a sound joint free from any pores, voids, and discontinuities has been obtained. It should be noted that the entire bonding

zone is much thicker than the 30 µm filler metal, proving that the dissolution of base alloys has occurred.

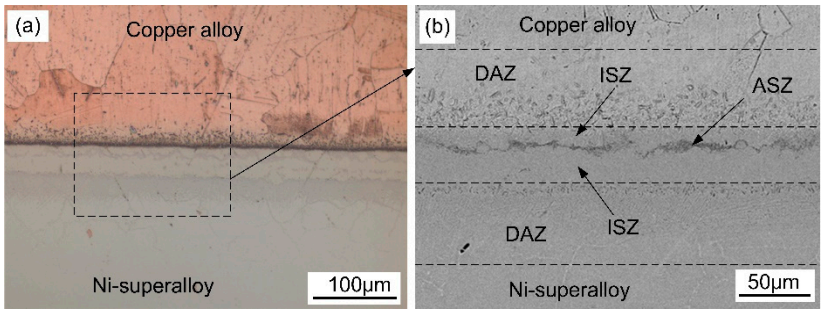

Figure 3. Optical (**a**) and SEM-BSE (**b**) micrographs of copper/superalloy interface in a TLP-bonded sample made at 1030 °C for 60 min.

Once the parts reach the bonding temperature, the interlayer melts and the melting point depressant (MPD) elements (B and Si) start diffusing into the copper alloy and nickel-based superalloy. The accumulation of these element leads to melting of both alloys and widening of the liquid phase until a compositional equilibrium is established. As further dissolution of the base materials continues, the concentration of MPD elements in the liquid goes down, and consequently, the melting point of the liquid phase increases. As soon as the liquidus temperature reaches the bonding temperature, isothermal solidification begins at the solid/liquid interface with a higher melting point, i.e., the superalloy/liquid interface in this case. If the holding time is not sufficiently long enough to complete isothermal solidification, the remaining liquid will form an athermally-solidified zone (ASZ) during the cooling stage.

A chemical analysis of the bond zone was conducted at several points of interest, and the results are shown in Figure 4 and Table 2.

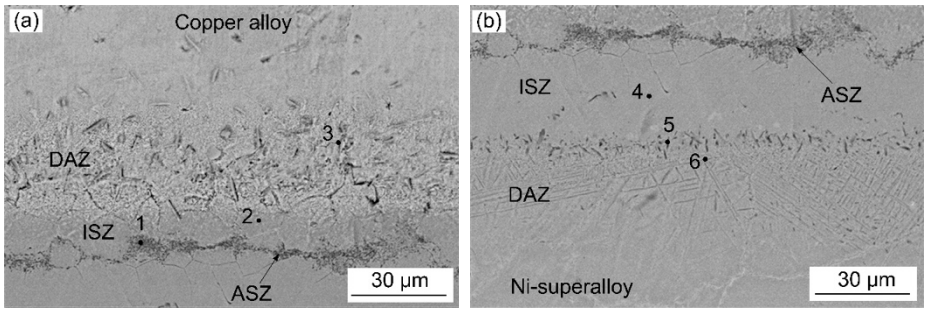

Figure 4. SEM micrographs of the copper side (**a**) and superalloy side (**b**) of a joint bonded for 60 min and the locations of EDS analyses.

Table 2. Chemical composition (wt. %) of various locations marked 1 to 6 in Figure 4.

Positions	Cu	Ni	Cr	Fe	Ti	Nb	Mo	Si	B
1	9.3	32.7	33.1	2.6	-	-	-	1.5	20.8
2	22.1	63.5	6.1	4.6	-	-	-	3.8	-
3	77.6	8.7	2.4	-	-	-	-	-	11.3
4	8.8	72.8	7.4	7.3	-	-	-	3.7	-
5	3.0	39	17.6	6.3	0.3		1.6	0.8	30.8
6	-	20	7.3	7.1	0.4	1.1	0.7	-	63.2

As seen in Table 2, the ASZ (point 1 in Figure 4a) is mostly a eutectic phase containing high amounts of boron. This is consistent with previous works, which showed that such eutectic microstructure comprises of Ni-boride, Ni-Si-B intermetallic, and γ solid solution in TLP-bonded Ni-based superalloys [21]. Furthermore, as shown in the EDS map (Figure 5b), the ASZ is enriched in Cr. According to the Cr-B phase diagram, various Cr-borides could be formed, including Cr_2B, Cr_5B_3, CrB, Cr_3B_4, CrB_2, and CrB_4. In addition, Cu was also found in the ASZ, which indicates the dissolution of base copper alloy at 1030 °C. Therefore, the eutectic phase found at ASZ contains Ni-borides, Cr-borides, and Ni-Cu solid solution.

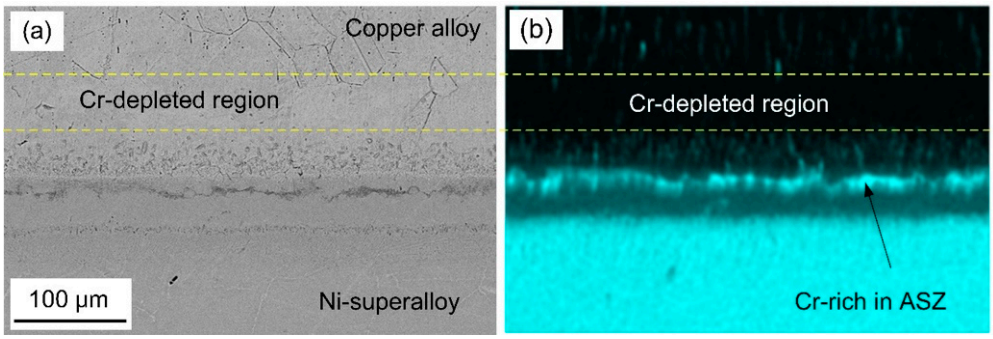

Figure 5. SEM-BSE image of the joint interface (**a**) and EDS elemental map of Cr (**b**). The ASZ is enriched in Cr whereas Cr-depleted region is formed in the DAZ of copper.

The ISZ close to copper consisted of a Ni-Cu solid solution with 63.5% Ni and 22.1% Cu (point 2 in Figure 4a), while the ISZ close to the nickel-superalloy consisted of Ni-Cu solid solution with 72.8% Ni and 8.8% Cu (point 4 in Figure 4b).

Since a high concentration of boron was detected on the grain boundaries in the DAZ of the copper side (point 3 in Figure 4a and Table 2), it is reasonable to assume that most of the boron diffused through the grain boundaries and into the copper.

The presence and morphology of the light-grey layer in Figure 4a indicates the formation and penetration of a liquid phase within the superalloy's grain boundaries—also known as "grain boundary wetting". In fact, grain boundary wetting is the main mechanism of gain boundary attack caused by liquid metals, e.g., severe disintegration of aluminium by liquid gallium in less than one minute [22]. Although, no grain boundary failure was observed in this work, it may occur when bonding other combinations of dissimilar alloys, particularly if the bonding time is not long enough.

It is also interesting to note that a Cr-depleted region was formed in the DAZ of copper (Figure 5). This is because Cr is a strong boride former [21], and the local depletion is the result of formation of various Cr borides in the DAZ adjacent to DAZ/ISZ interface. The concentration of Cr in this region is 2.4%, which is higher than 0.8% in the parent copper alloy.

The microstructure of the TLP bonded Ni-based superalloy is well studied [7,12,18,21,23], and most of the reported features, such as needle-like borides precipitates, were also found at the ISZ/DAZ interface and DAZ of the sample examined in this work (points 5 and 6 in Figure 4b).

Figure 6 shows the linear concentration profiles of main elements. Sudden changes in the concentration of Ni and Cr in the ASZ and DAZ close to the copper alloy are mainly due to the formation of Cr-rich borides. It should also be noted that more Ni diffused into the copper alloy than Cu into the Ni superalloy.

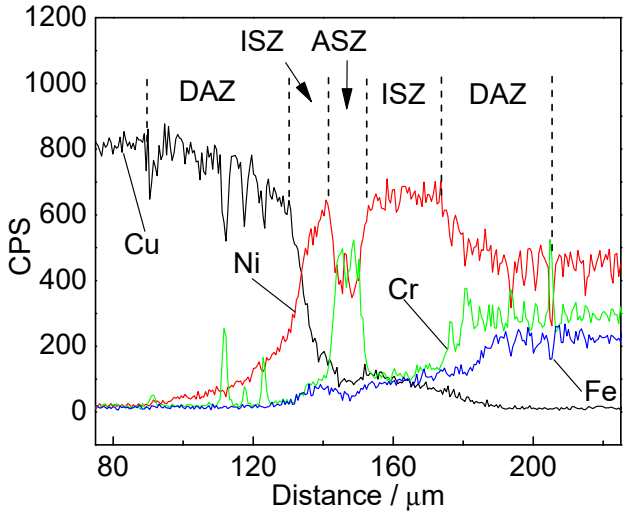

Figure 6. Concentration profiles of main elements across the joint interface of a sample bonded for 60 min.

The effect of bonding time on the microstructures of the bonding zone is shown in Figure 7. With increasing the bonding time, the amounts of eutectic phases in ASZ decreased and the width of ISZ increased. No eutectic phases or needle-shape borides were found in the ISZ of the sample bonded at 1030 °C for 90 min, which indicated the completion of isothermal solidification. As expected, boron diffuses deeper into the base alloys, and more uniform DAZ is formed with increasing bonding time. Nevertheless, the borides still exist in the DAZ of the copper alloy. More effective homogenization treatment should be developed to obtain a more uniform distribution of such precipitates on both sides.

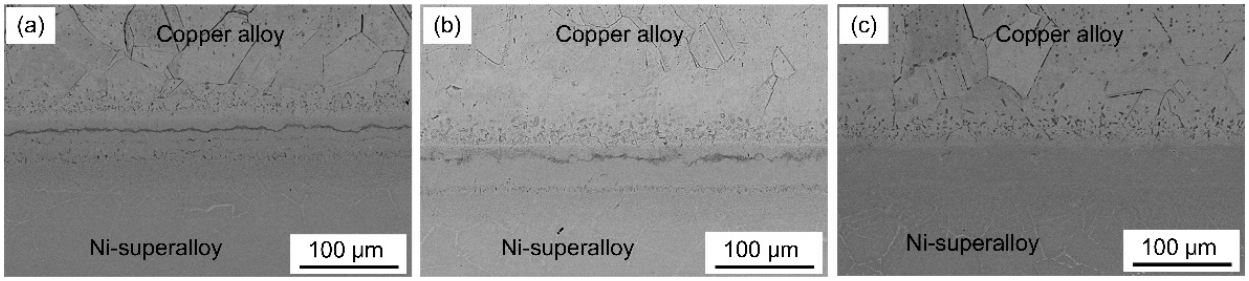

Figure 7. Microstructures of samples TLP-bonded within different bonding times: (**a**) 30 min, (**b**) 60 min, and (**c**) 90 min. Complete isothermal solidification was obtained when bonding at 1030 °C for 90 min.

3.2. Tensile Strength and Microhardness Distribution

Two samples were bonded in three bonding conditions (6 in total), and of each set, one sample was tensile tested (3 in total). All of the tensile-tested samples failed in the copper alloy, indicating that their bond strengths were above the ultimate tensile strength (UTS) of the copper alloy (Figure 2). The ultimate tensile strength of the samples bonded at 30, 60, and 90 min were 268, 292, and 272 MPa, respectively. The variation in the tensile strengths is within experimental error.

Figure 8 shows the hardness distributions across the bonding zone in the samples made within various bonding times. A sharp peak in hardness was found only in the samples bonded for 30 min. Since the bonding time was not sufficient to complete the isothermal solidification, the formation of very hard intermetallics (IMCs) in the ASZ is expected.

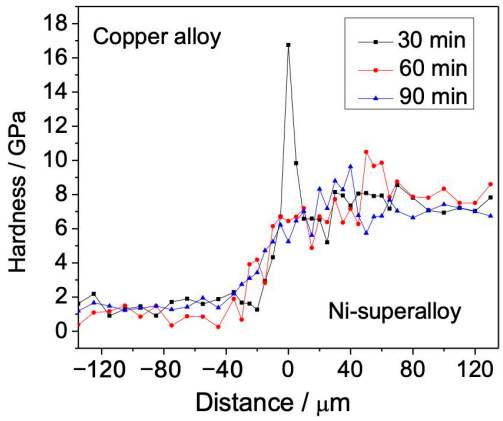

Figure 8. Effect of bonding time on the hardness distributions of samples bonded at 1030 °C.

The hardness gradually increased from the copper alloy to the bond zone, as the concentration of Ni in the copper alloy changed—see Figure 6. Some elements from the interlayer diffused into the copper alloy and consequently resulted in an increase of the hardness in the DAZ on the copper side.

4. Conclusions

Transient Liquid Phase (TLP) bonding of a copper alloy to a nickel-based superalloy using BNi-2 interlayer was performed in a vacuum. Based on the results of the microstructural examinations and mechanical testing, the following conclusions were made:

1. Three different zones were formed in a joint made at 1030 °C for 60 min: an isothermal solidification zone (ISZ) containing Cu-Ni solid solutions on both sides; an athermal solidification zone (ASZ), which was identified by the presence of eutectic phase; and a diffusion affected zone (DAZ) located further away from the joint.
2. Full isothermal solidification was achieved when bonding was performed at 1030 °C for 90 min.
3. All of the tensile-tested samples failed in the copper alloy and away from the joints regardless of bonding times of 30, 60, and 90 min.
4. Excluding some sharp peaks in the hardness profile due to the formation of intermetallics, the hardness gradually increases from the copper alloy to the nickel-based superalloy.

Author Contributions: Conceptualization, C.Z. and A.S.; methodology, C.Z.; validation, C.Z. and A.S.; formal analysis, C.Z. and A.S.; investigation, C.Z. and A.S.; resources, C.Z.; data curation, C.Z. and A.S.; writing—original draft preparation, C.Z.; writing—review and editing, C.Z. and A.S.; visualization, C.Z.; supervision, C.Z. and A.S.; project administration, C.Z.; funding acquisition, C.Z. All authors have read and agreed to the published version of the manuscript.

Funding: This research was funded by the National Natural Science Foundation of China, grant number 51905348. The first author was sponsored by the Shanghai Rising-Star Program, grant number 20QB1402700.

Institutional Review Board Statement: Not applicable.

Informed Consent Statement: Not applicable.

Data Availability Statement: The data presented in this study are available on request from the corresponding author.

Acknowledgments: The authors would like to acknowledge the technical assistance and helpful discussion received from Chunsheng Sha, Zhijun Li, and Cheng Xu.

Conflicts of Interest: The authors declare no conflict of interest.

References

1. Goods, S.H.; Puskar, J.D. Solid state bonding of CuCrZr to 316L stainless steel for ITER applications. *Fusion Eng. Des.* **2011**, *86*, 1634–1638. [CrossRef]
2. Lee, H.S. Diffusion Bonding of Metal Alloys in Aerospace and Other Applications. In *Welding and Joining of Aerospace Materials*; Woodhead Publishing Limited: Sawston, UK, 2012; pp. 320–344.
3. Sabetghadam, H.; Hanzaki, A.Z.; Araee, A. Diffusion bonding of 410 stainless steel to copper using a nickel interlayer. *Mater. Charact.* **2010**, *61*, 626–634. [CrossRef]
4. Batra, I.S.; Kale, G.B.; Saha, T.K.; Ray, A.K.; Derose, J.; Krishnan, J. Diffusion bonding of a Cu-Cr-Zr alloy to stainless steel and tungsten using nickel as an interlayer. *Mater. Sci. Eng. A* **2004**, *369*, 119–123. [CrossRef]
5. Singh, K.P.; Patel, A.; Bhope, K.; Khirwadkar, S.S.; Mehta, M. Optimization of the diffusion bonding parameters for SS316L/CuCrZr with and without Nickel interlayer. *Fusion Eng. Des.* **2016**, *112*, 274–282. [CrossRef]
6. Zhang, C.; Shirzadi, A.A. Diffusion bonding of copper alloy to nickel-based superalloy: Effect of heat treatment on the microstructure and mechanical properties of the joints. *Sci. Technol. Weld. Join.* **2021**, *26*, 213–219. [CrossRef]
7. Jamaloei, A.D.; Khorram, A.; Jafari, A. Characterization of microstructure and mechanical properties of dissimilar TLP bonding between IN718/IN600 with BNi-2 interlayer. *J. Manuf. Process.* **2017**, *29*, 447–457. [CrossRef]
8. Liu, M.c.; Sheng, G.m.; He, H.j.; Jiao, Y.j. Microstructural evolution and mechanical properties of TLP bonded joints of Mar-M247 superalloys with Ni-Cr-Co-W-Ta-B interlayer. *J. Mater. Process. Technol.* **2017**, *246*, 245–251. [CrossRef]
9. Hadibeyk, S.; Beidokhti, B.; Sajjadi, S.A. The effect of interlayer thickness, bonding temperature and atmosphere on transient liquid phase bonding of GTD-111 to FSX-414. *J. Mater. Process. Technol.* **2018**, *255*, 673–678. [CrossRef]
10. Alhazaa, A.; Haneklaus, N. Diffusion bonding and transient liquid phase (TLP) bonding of type 304 and 316 austenitic stainless steel—A review of similar and dissimilar material joints. *Metals* **2020**, *10*, 613. [CrossRef]
11. Jing, Y.; Zheng, Z.; Liu, E.; Guo, Y. Microstructural Evolution of a Ni-base Alloy DZ468 Joint Bonded with a New Co-base Filler. *J. Mater. Sci. Technol.* **2014**, *30*, 480–486. [CrossRef]
12. Abbasi-Khazaei, B.; Jahanbakhsh, A.; Bakhtiari, R. TLP bonding of dissimilar FSX-414/IN-738 system with MBF-80 interlayer: The effect of homogenizing treatment on microstructure and mechanical properties. *Mater. Sci. Eng. A* **2016**, *651*, 93–101. [CrossRef]
13. Binesh, B.; Gharehbagh, A.J. Transient Liquid Phase Bonding of IN738LC/MBF-15/IN738LC: Solidification Behavior and Mechanical Properties. *J. Mater. Sci. Technol.* **2016**, *32*, 1137–1151. [CrossRef]
14. Kim, J.K.; Park, H.J.; Shim, D.N.; Kim, D.J. Effect of bonding parameters on microstructural characteristics during TLP bonding of directionally solidified Ni-based superalloy. *J. Manuf. Process.* **2017**, *30*, 208–216. [CrossRef]
15. Hadibeyk, S.; Beidokhti, B.; Sajjadi, S.A. Effect of bonding time and homogenization heat treatment on the microstructure and mechanical properties of the transient liquid phase bonded dissimilar GTD-111/FSX-414 TLP superalloys. *J. Alloys Compd.* **2018**, *731*, 929–935. [CrossRef]
16. Azqadan, E.; Ekrami, A. Transient liquid phase bonding of dual phase steels using Fe-based, Ni-based, and pure Cu interlayers. *J. Manuf. Process.* **2017**, *30*, 106–115. [CrossRef]
17. Esmaeili, H.; Mirsalehi, S.E.; Farzadi, A. Vacuum TLP bonding of Inconel 617 superalloy using Ni-Cr-Si-Fe-B filler metal: Metallurgical structure and mechanical properties. *Vacuum* **2018**, *152*, 305–311. [CrossRef]
18. Pouranvari, M.; Ekrami, A.; Kokabi, A.H. Transient liquid phase bonding of wrought IN718 nickel based superalloy using standard heat treatment cycles: Microstructure and mechanical properties. *Mater. Des.* **2013**, *50*, 694–701. [CrossRef]
19. Bakhtiari, R. Effect of configuration and composition of interlayer on TLP joints of FSX-414 superalloy. *J. Mater. Process. Technol.* **2016**, *231*, 8–17. [CrossRef]
20. Shamsabadi, A.Y.; Bakhtiari, R.; Eisaabadi, B.G. TLP bonding of IN738/MBF20/IN718 system. *J. Alloys Compd.* **2016**, *685*, 896–904. [CrossRef]
21. Pouranvari, M.; Ekrami, A.; Kokabi, A.H. Solidification and solid state phenomena during TLP bonding of IN718 superalloy using Ni-Si-B ternary filler alloy. *J. Alloys Compd.* **2013**, *563*, 143–149. [CrossRef]
22. Shirzadi, A.A.; Saindrenan, G. New method for flux free diffusion brazing of aluminium alloys using liquid gallium (UK patent application 0128623.6). *Sci. Technol. Weld. Join.* **2003**, *8*, 149–153. [CrossRef]
23. Zhang, L.X.; Sun, Z.; Xue, Q.; Lei, M.; Tian, X.Y. Transient liquid phase bonding of IC10 single crystal with GH3039 superalloy using BNi2 interlayer: Microstructure and mechanical properties. *Mater. Des.* **2016**, *90*, 949–957. [CrossRef]